

Intrinsic phase fluctuation and superfluid density in doped Mott insulators

Zeyu Han,^{1,*} Zhi-Jian Song,^{1,*} Jia-Xin Zhang,^{2,3,1} and Zheng-Yu Weng¹

¹*Institute for Advanced Study, Tsinghua University, Beijing 100084, China*

²*French American Center for Theoretical Science, CNRS,*

KITP, Santa Barbara, California 93106-4030, USA

³*Kavli Institute for Theoretical Physics, University of California, Santa Barbara, California 93106-4030, USA*

(Dated: March 27, 2025)

The doping dependence of the superfluid density ρ_s exhibits distinct behaviors in the underdoping and overdoping regimes of the cuprate, while the superconducting (SC) transition temperature T_c is generally scaled with ρ_s . In this paper, we present a unified understanding of the superconducting transition temperature T_c and ρ_s across the entire doping range by incorporating the underlying mutual Chern-Simons gauge structure that couples the spin and charge degrees of freedom in the doped Mott insulator. Within this framework, the SC phase fluctuations are deeply intertwined with the spin dynamics, such that thermally excited neutral spins determine T_c , while quantum spin excitations effectively reduce the superfluid density at zero temperature. As a result, a Uemura-like scaling of T_c vs. ρ_s in the underdoped regime naturally emerges, while the suppression of both T_c and ρ_s at overdoping is attributed to a drastic reduction of antiferromagnetic spin correlations.

Introduction.— One of the key distinctions between the cuprate superconductor and a conventional BCS superconductor lies in the conjecture that the superconducting (SC) phase transition be controlled by superfluid density in the former instead of the Cooper pairing strength in the latter [1–3]. It is experimentally supported by the scaling of T_c with the superfluid density as discovered by Uemura *et al.* [4–6]. Here strong SC phase fluctuations is generally expected with weak phase stiffness due to small superfluid density, which may be realized at low density of charge carriers in doped Mott insulators [3, 7]. However, a Kosterlitz-Thouless (KT)-type transition temperature with such low superfluid density still predicts a much higher T_c using reasonable parameters from the cuprate [3, 8, 9], and the issue why a realistic T_c is so low remains an important puzzle for a high- T_c theory based on the doped Mott insulator description.

The scaling behavior of T_c with the superfluid density persists even into overdoping [10], where both turn to decreasing and eventually vanishing with the continuous increase of doping concentration. It challenges a prevailing conjecture that the cuprate become a conventional BCS superconductor with reducing pairing strength in the overdoping, as the emergence of a large Fermi surface [11, 12] may indicate a reduction in electronic correlations. In order to explain the missing superfluid density based on the BCS theory, some theoretical work has attributed it to strong scattering or disorder effects [13–16]. However, in addition to the suppression of T_c and superfluid stiffness, various anomalies still persist, which are of non-BCS nature [17]. The presence of the in-gap states observed by ARPES [18] and the gap-filling seen in STM studies [19] both indicate that phase fluctuations continue to play a significant role in driving the SC transition. The resonance-like low-energy spin mode is still present in the SC region [20–23]. At high temperatures, the strange metal behavior has been observed across the

doping range, from the underdoped to the overdoped side [24]. A great deal of experimental evidence seems to point to a unified SC dome bounded by the anomalous phase fluctuations that call for a consistent theory.

In this paper, we discuss an unconventional phase fluctuation that can crucially influence the SC transition temperature T_c and the superfluid density ρ_s in doped Mott insulators. In the conventional slave-boson mean-field theory [3, 9] of the d-wave SC state in the t - J model, the ground state is depicted by a Bose condensate of spinless holons in a short-range AFM ordered or resonating-valence-bond (RVB) spin background, with T_c coinciding with the holon condensation temperature T_v^0 . However, in the phase-string formalism [25] of the t - J model, it is found that the holon condensate can further perceive a strong phase frustration from the RVB background if a spin-singlet RVB pair is broken into independent $S = 1/2$ spinons in the latter. Here, T_c and ρ_s can be substantially renormalized, respectively, by such a phase fluctuation that is excited thermally or quantum mechanically. A generalized Uemura plot is obtained in the whole doping regime, which also naturally explains the suppression of both T_c and ρ_s in the overdoped regime as the destruction of the short-range AFM correlation.

Key results.—Phase diagram in Fig. 1 illustrates the overall evolution of the half-filling AFM phase upon doping (with doping concentration δ), based on the mutual Chern-Simons (MCS) gauge theory [25, 26], in which the SC phase (white-colored dome) is the main focus of the present work. Here the MCS gauge structure refers to an intrinsic sign structure known as the phase string effect in the t - J model [28–30], due to the opening of the Mott gap. This gauge structure is equivalent to that the spins as local moments and holes as dopants perceive each other as π -flux solenoids as illustrated in Fig. 2 (a). Thus, the spin and charge degrees of freedom are intrinsically long-range entangled via an Aharonov-Bohm effect

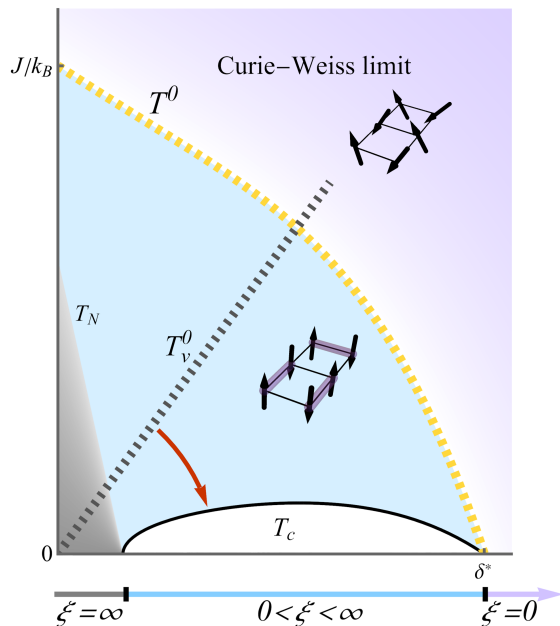


FIG. 1. The phase diagram for a doped Mott insulator based on the mutual Chern-Simons (MCS) gauge description. The low-temperature white-colored dome indicates the superconducting phase, of which T_c is drastically reduced from a bare T_v^0 by the MCS gauge fluctuations. Here the phase coherence is protected by spin local moments forming the bosonic RVB pairing with a finite spin-spin correlation length ξ . Self-consistently the antiferromagnetic long-range order (bounded by the Neel temperature T_N with a divergent ξ in the gray area) gets quickly destroyed by doped holes and evolves into a short-range ordered phase bounded by T_0 (the blue area), which is further connected to a purple-colored overdoped regime with the Curie-Weiss-like paramagnetic phase of vanishing ξ at doping $\delta^* \simeq 0.26$ [26].

to mutually exert gauge interactions [29, 30].

At finite doping, the holon condensate will quickly destroy the long-range AFM order such that the low-lying spin-wave excitation around (π, π) becomes a nonpropagating/resonance-like mode at the Schwinger-boson mean-field level with a gap E_g as shown in Fig. 2 (b). At finite temperature, thermally excited spins will then cause strong frustrations on the charge condensate via the MCS gauge field depicted in Fig. 2(a). In contrast to a bare holon condensation (KT-like) temperature $T_v^0 \simeq \rho_s^0 \propto \delta t$ (cf. Fig. 1), the real SC phase is brought down as illustrated by the white-colored dome. Specifically, T_c is essentially determined by E_g as follows

$$T_c \simeq \frac{E_g}{6.44k_B}, \quad (1)$$

which shows an excellent agreement with the cuprate superconductors in Fig. 2(c), where the resonance energy E_g is either taken from the neutron scattering or Raman scattering measurements [27].

By the same MCS gauge fluctuation, the superfluid density is renormalized by the spin excitations at $T = 0$ as follows:

$$\rho_s = \rho_s^0 \frac{\lambda E_g}{\lambda E_g + \rho_s^0}, \quad (2)$$

where $\lambda \simeq 1/(2\pi^2)$ is a numerical constant based on the mean-field calculation. Again the spin resonance energy E_g plays a crucial role here in the renormalization of the superfluid density. Only in the limit of large E_g can the bare ρ_s^0 be restored as the stiffness for the phase fluctuations of the holon condensate. In the opposite limit of $E_g \rightarrow 0$, $\rho_s \rightarrow \lambda E_g$ similar to the T_c in Eq. (1). Thus, the ratio of T_c and ρ_s is generally expected to be a constant $O(1)$ on the two sides of the SC dome. The detailed T_c and ρ_s vs. doping δ are shown in Fig. 3 (a). A generalized Uemura plot of T_c vs. ρ_s is then obtained in Fig. 3 (b).

As summarized in Fig. 1, the SC phase is composed of the holon condensate and the spin RVB state in the white-colored region, which is self-consistently protected by an emergent resonance-like spin gap E_g with a finite spin-spin correlation length ξ . Above T_c given in Eq.(1), the thermally excited (deconfined) spinons in the MCS gauge theory destroy the SC phase coherence, giving rise to strong SC phase fluctuations between $T_c < T < T_v^0$. Here, both T_c and superfluid density vanish as $E_g \rightarrow 0$ with a divergent ξ approaching the AFM ordered phase in underdoping. In contrast, both T_c and the superfluid density also vanish near $\delta = \delta^*$ ($T = 0$) or $T = T_0$ in overdoping, as shown in Fig. 4, which corresponds to the collapse of the bosonic RVB state with $\xi \rightarrow 0$ and $E_g \rightarrow 0$. Thus, the novel collective fluctuations of the MCS gauge fields, beyond the Schwinger-boson mean-field description, systematically decide the low-temperature phase diagram upon doping.

Mutual Chern-Simons gauge theory of the doped Mott insulator.— The minimal MCS field-theory description of the mutual π -flux attachments [31–33], based on the phase-string formulation [25, 29] of the t - J model, is governed by the lattice Euclidean Lagrangian $L = L_h + L_s + L_{\text{MCS}}$ as follows:

$$L_h = \sum_i h_i^\dagger [\partial_0 - iA_0^s(i) - iA_0^e(i) + \mu_h] h_i - t_h \sum_{i\alpha} \left[h_i^\dagger h_{i+\alpha} e^{iA_\alpha^s(i) + iA_\alpha^e(i)} + \text{h.c.} \right], \quad (3)$$

$$L_s = \sum_{i\sigma} b_{i\sigma}^\dagger [\partial_0 - i\sigma A_0^h(i) + \lambda_b] - J_s \sum_{i\alpha\sigma} \left[b_{i\sigma}^\dagger b_{i+\alpha, \bar{\sigma}} e^{i\sigma A_\alpha^h(i)} + \text{h.c.} \right], \quad (4)$$

$$L_{\text{MCS}} = \frac{i}{\pi} \sum_i \epsilon^{\mu\nu\lambda} A_\mu^s(i) \partial_\nu A_\lambda^h(i), \quad (5)$$

in which L_h and L_s describe the dynamics of the matter fields — bosonic spinless holon h_i , and bosonic neutral

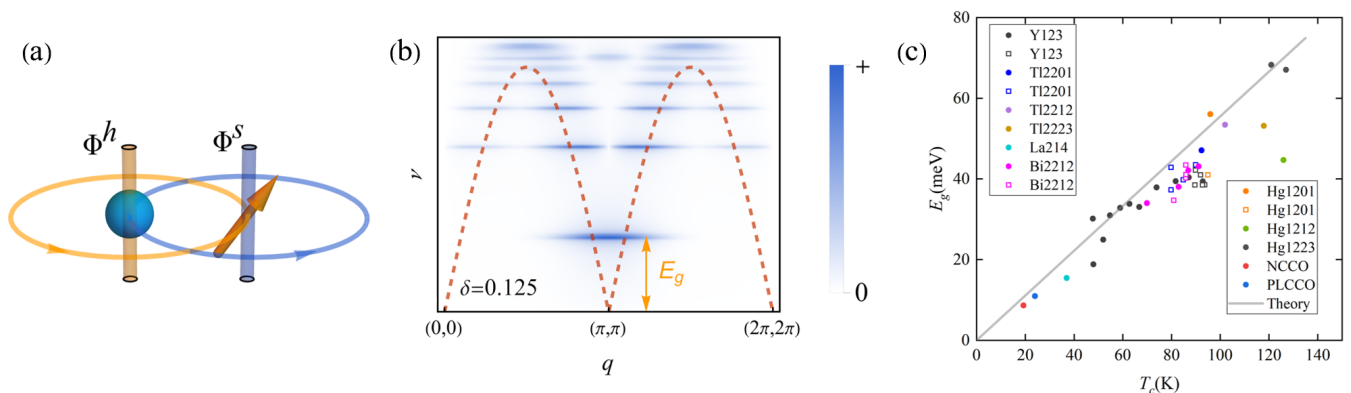


FIG. 2. (a) Intrinsic phase fluctuations arise from the long-range spin-charge entanglement in the MCS gauge theory: A holon carries a π -flux $\Phi^h \equiv \pm\pi n^h$ as perceived by a spinon of spin index $\sigma = \pm 1$, and *vice versa*, a spinon carries a flux $\Phi^s \equiv \pi \sum_{\sigma} \sigma n_{\sigma}^b$ seen by holons; (b) A finite density of holons reshapes the $S = 1$ spin excitation spectrum into a resonance-like mode at energy E_g near antiferromagnetic wavevector (π, π) at the mean-field level (with $\delta = 0.125$); (c) The superconducting critical temperature T_c according to (1), with the experimental data replotted from [27].

spinon $b_{i\sigma}$ (with $\bar{\sigma} \equiv -\sigma$), respectively. The indices α and β denote only the spatial components: x, y , and the indices $\mu = (\tau, \mathbf{r})$ label the full time-space vector. λ_b and μ_h are the chemical potentials for the spinon b and holon h , whose numbers are conserved. The hole doping concentration δ will be introduced via μ_h . The renormalized hopping strength t_h and effective spin AFM coupling J_s are determined at a generalized mean-field level in Ref. 26. The external electromagnetic vector potential A^e with a field strength B^e perpendicular to the 2D plane appears in Eq. (3) for the charge (holon) degree of freedom (setting the charge equal to one).

Here the holon field h and spinon field b_{σ} minimally couple to the gauge fields, A_{μ}^s and A_{μ}^h , respectively, which are entangled by the MCS topological term in Eq. (5). The strengths of these MCS fields are determined by the following equations of motion for A_0^s and A_0^h , respectively:

$$\epsilon^{\alpha\beta} \partial_{\alpha} A_{\beta}^h \equiv B^h = \pi n^h, \quad (6)$$

$$\epsilon^{\alpha\beta} \partial_{\alpha} A_{\beta}^s \equiv B^s = \pi \sum_{\sigma} \sigma n_{\sigma}^b. \quad (7)$$

Namely, the holon (spinon) number n^h (n^b) will determine the gauge-field strength of A_{μ}^h (A_{μ}^s) as if each matter particle (holon or spinon) is attached to a fictitious π flux solenoid visible only by a distinct species as illustrated in Fig. 2(a).

A. Emergent bosonic RVB as a short-range AFM state.—At half-filling, the action L will reduce to L_s in (4) in the Schwinger-boson mean-field state with $n^h = B^h = 0$. It well describes the AFM phase with $T_0 \sim J/k_B$ denoting the onset temperature of the short-range AFM correlation. Upon doping, a finite flux B^h will be perceived by the spinons in Eq.(4) according to Eq.(6), which can drastically modify the spin dynamics as illustrated in Fig. 2(b) calculated self-consistently at the *bosonic* RVB mean-field level (cf. Ref. 26). It shows that the low-lying

gapless spin wave excitation (dashed curve) is replaced by a prominent “resonance-like” mode with gap E_g around the AFM wavevector (π, π) , while the high-energy excitations are dispersed into non-propagating weaker incoherent modes. Namely, an AFM ordered spin background at half-filling can be turned into a short-range AFM due to the flux-binding effect. A systematic evolution of the spin correlations/dynamics as a function of doping is schematically illustrated in Fig. 1, in which the inherited Schwinger-boson-like bosonic RVB order parameter, characterizing the short-range AFM order at $T \leq T_0$, will get continuously suppressed with increasing doping. It eventually terminates at some overdoped concentration $\delta^* \simeq 0.26$ at zero temperature or a finite T_0 , beyond which a Curie-Weiss-like paramagnetic phase sets [26] in.

B. Superconducting phase coherence.— The condensed charge (holons) would remain SC phase coherent below T_v^0 , as far as the external A^e perceives, if the internal gauge field $A^s \equiv 0$ in Eq. (3). Here T_v^0 denotes the conventional KT transition temperature for a 2D hard-core holon gas with a bare superfluid density ρ_s^0 . Without A^s , T_v^0 would be too high as a realistic T_c in the slave-boson RVB theory [8, 9]. However, in the present MCS theory, T_c can be drastically reduced by the fluctuation of A^s , which describes the π -flux-tubes associated with individual spins in the background according to Eq.(7). Note that in the RVB ground state, A^s remains canceled to ensure the phase coherence without generating net fluxes according to Eq. (7).

On the other hand, once the spinons are thermally excited by breaking up the RVB pairs in Eq.(4), their associated π fluxes in A^s eventually can proliferate by a confinement-deconfinement transition, which results in a non-SC phase full of composite spinon- π -vortices in the holon condensate described by L_h in Eq. (3). Such a

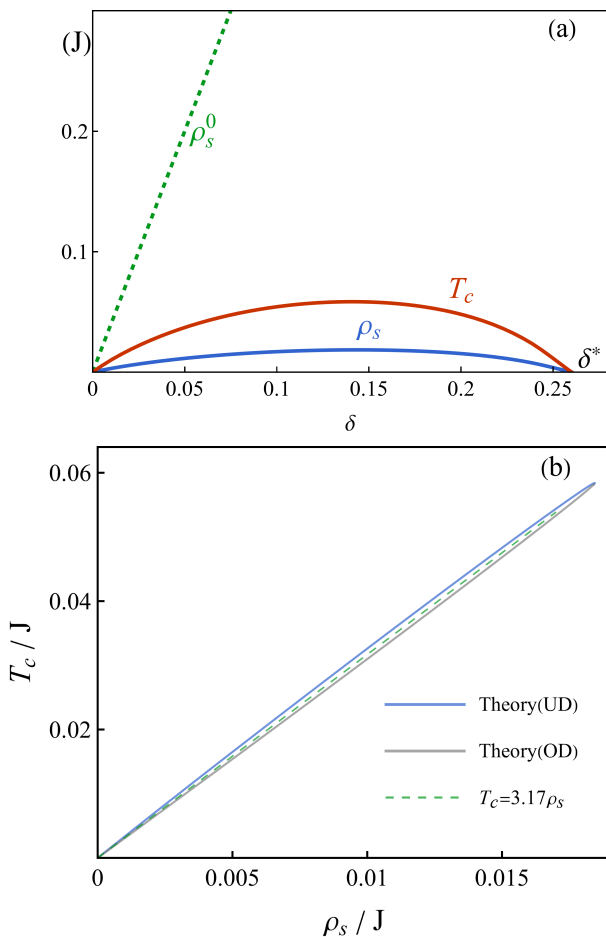


FIG. 3. (a) Bare superfluid density ρ_s^0 , renormalized superfluid density ρ_s , and superconducting transition temperature T_c versus doping concentration δ , where $\delta^* \approx 0.26$ denotes the superconducting ending point. The underlying parameters are the same as used at the mean-field level in Ref. 26; (b) T_c versus ρ_s , where the blue curve and gray curve represents the underdoped (UD) (with $\delta < 0.14$) and overdoped (OD) (with $\delta > 0.14$) regimes, respectively. The green dashed line indicates the fitting of $T_c = 3.17\rho_s$.

strong SC fluctuating state is known as the lower pseudogap phase. The corresponding phase transition T_c can be obtained according to a renormalization group calculation (cf. Refs. 27 and 34 and Appendix C), which is essentially determined by the low-lying spin resonance energy E_g as given in Eq. (1). The universal scaling law of the T_c formula in Eq. (1) is illustrated in Fig. 2(c), alongside the experimental data obtained by neutron scattering and Raman scattering measurements [27]. As noted above, E_g as a function of doping is calculated by a self-consistent mean-field approach, which determines T_c via Eq. (1) as shown in Fig. 3.

C. Superfluid stiffness at zero temperature.— The superfluid density ρ_s will characterize the response of the SC phase to an applied external gauge field A^e . According to Eq. (3), the holon condensate is coupled to both

the external A^e and an internal topological gauge field A^s , respectively, and the latter should be integrated out in order to determine the renormalized ρ_s . According to the relation Eq. (7), the flux strength B^s for A^s is tied to the spin excitations such that A^s is governed by the dynamical spin correlation as follows

$$D_{\alpha\beta}^{A^s}(\mathbf{q}, i\omega) \equiv \langle A_\alpha^s A_\beta^s \rangle = \delta_{\alpha\beta} \frac{4\pi^2}{q^2 a^4} \chi^{zz}(\mathbf{q}, i\omega). \quad (8)$$

Here $\chi^{zz} = \langle S^z S^z \rangle$ represents the dynamical spin susceptibility calculated based on the b-spinon Lagrangian L_s in Eq. (4) at the mean-field level, given by

$$\lim_{q \rightarrow 0} \frac{4\pi^2}{q^2 a^2} \chi^{zz}(\mathbf{q}, i\omega) \simeq \frac{1}{\lambda E_g}, \quad (9)$$

in the long-wavelength limit with λ of order $O(1/(2\pi^2))$ as detailed in Appendix B.

In the SC state, by expressing $h_i = \sqrt{n^h} e^{i\theta_i^h}$ for the holon condensate, the effective Lagrangian may be rewritten in the continuous limit as follows

$$L_{\text{eff}} = \frac{1}{2} \int_0^\beta d\tau \int d\mathbf{r} [\rho_s^0 (\partial_\alpha \theta^h - A_\alpha^s - A_\alpha^{\text{ext}})^2 + \lambda E_g A_\alpha^s{}^2] \quad (10)$$

where we have incorporated an effective term for the internal gauge field A^s after integrating out the b -spinons as discussed above. Subsequently the equation of motion gives rise to $A_\alpha^s = -\frac{\rho_s^0}{\rho_s^0 + \lambda E_g} A_\alpha^e$ ($\rho_s^0 \equiv 2t_h n^h$), resulting in

$$L_{\text{eff}} = \int d\mathbf{r} \frac{\rho_s}{2} (A^e)^2 \quad (11)$$

where ρ_s is given in Eq. (2) (cf. Appendix A for details).

As shown in Fig. 3(a), T_c and ρ_s are strongly renormalized by the spin resonance energy E_g , with ρ_s substantially reduced from the bare value ρ_s^0 . Especially in the overdoping regime, the doping dependence of ρ_s (cf. Fig. 4) reverses from ρ_s^0 to decrease and terminate at δ^* , which explains the experimental data from the experiments of Bozovic et al. [10]. Note that $\rho_s^0 = 4\delta J$ is used by taking $t_h = 2J$ [26], which can also be regarded an independent phenomenological parameter, in addition to λE_g in Eq. (2). Finally, in $E_g \rightarrow 0$ in the two limits of under- and overdoping, the corrections from higher energy levels [cf. Fig. 2(b)] to both T_c and ρ_s may become important, which is beyond the present approach.

Discussion.— In this work, we have shown that the spin excitations are fundamentally entangled with the charge phase fluctuations in a doped Mott insulator by the MCS gauge structure. The latter comes from the phase-string sign structure of the t - J model or the Hubbard model with the opening of the Mott gap. At low doping, although the spin local moments can far exceed the doped holes in numbers, the AFM order can

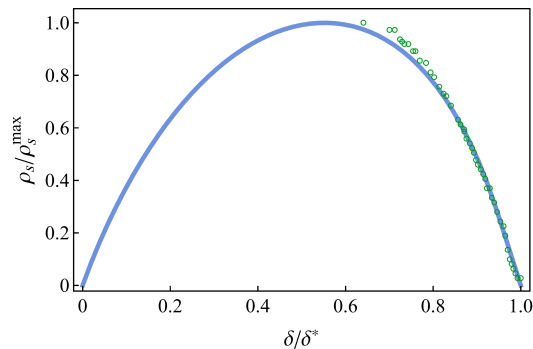


FIG. 4. Experimentally observed superfluid density (open circle) is suppressed in the overdoped regime, which is well fit by the rescaled ρ_s/ρ_s^{\max} vs doping δ/δ^* , where ρ_s^{\max} denotes the maximal ρ_s shown in Fig. 3(a). The experimental data are taken from Bozovic et al. [10].

be quickly destroyed by the motion of the latter via the MCS field to result in a short-range AFM-ordered state, characterized by a resonance-like gap E_g . In turn, charge coherence is strongly influenced by low-lying spin excitations at E_g via MCS gauge fluctuations as “cheap vortices”, which decide the superconducting critical temperature T_c and zero-temperature superfluid density ρ_s . Here, the relations between T_c , ρ_s , E_g , as well as their general doping dependence, are generally consistent with the cuprate superconductor.

Therefore, the phase diagram discussed in this work is emergent, in which both spin resonance-like excitation and SC phase coherence are all parts of a self-organized low-temperature phenomenon upon doping the Mott insulator. At a high temperature above T_0 or doping beyond δ^* at $T = 0$ (cf. Fig. 1), the bosonic RVB state with the mean field coupling J_s is melt in Eq. (4) such that one enters the Curie-Weiss paramagnetic phase, where a substantially strong scattering to the charge degree of freedom by the MCS gauge fluctuation is expected [35] to result in a strange metal behavior. Furthermore, in addition to the b -spinon in the MCS Lagrangian L , an itinerant spinon associated with the backflow of holons will appear at higher energies [25, 26, 36]. Incorporating the latter can give rise to an hourglass-like dispersion [36] in replacing the spin resonance mode in Fig. 2(b) at the RPA level, consistent with inelastic neutron scattering experiments [37, 38]. But T_c will still be determined by the resonance mode at E_g which becomes the lower branch of the hourglass excitation [36]. Finally, the AFM order with $E_g = 0$ and $T_c = 0$ persisting in the lightly doped regime [31] of Fig. 1) will be further explored elsewhere.

We acknowledge stimulating discussions with Zhi-Long Wang. The financial support by MOST of China (Grant No. 2021YFA1402101) and NSF of China (Grant No. 12347107) is acknowledged. J.X.Z was funded by the European Research Council (ERC) under the European Union’s Horizon 2020 research and innovation program

(Grant Agreement No. 853116, acronym TRANSPORT): J.X.Z was also supported in part by grant NSF PHY-2309135 to the Kavli Institute for Theoretical Physics (KITP).

* These authors contributed equally to this work.

- [1] V. J. Emery and S. A. Kivelson, Importance of phase fluctuations in superconductors with small superfluid density, *Nature* **374**, 434 (1995).
- [2] E. W. Carlson, V. J. Emery, S. A. Kivelson, and D. Orgad, Concepts in high temperature superconductivity, in *Superconductivity: Conventional and Unconventional Superconductors*, edited by K. H. Bennemann and J. B. Ketterson (Springer Berlin Heidelberg, Berlin, Heidelberg, 2008) pp. 1225–1348.
- [3] P. A. Lee, N. Nagaosa, and X.-G. Wen, Doping a mott insulator: Physics of high-temperature superconductivity, *Rev. Mod. Phys.* **78**, 17 (2006).
- [4] Y. J. Uemura, G. M. Luke, B. J. Sternlieb, J. H. Brewer, J. F. Carolan, W. N. Hardy, R. Kadono, J. R. Kempton, R. F. Kiefl, S. R. Kreitzman, P. Mulhern, T. M. Riseman, D. L. Williams, B. X. Yang, S. Uchida, H. Takagi, J. Gopalakrishnan, A. W. Sleight, M. A. Subramanian, C. L. Chien, M. Z. Cieplak, G. Xiao, V. Y. Lee, B. W. Statt, C. E. Stronach, W. J. Kossler, and X. H. Yu, Universal correlations between T_c and $\frac{\rho_s}{m^*}$ (carrier density over effective mass) in high- T_c cuprate superconductors, *Phys. Rev. Lett.* **62**, 2317 (1989).
- [5] Y. J. Uemura, L. P. Le, G. M. Luke, B. J. Sternlieb, W. D. Wu, J. H. Brewer, T. M. Riseman, C. L. Seaman, M. B. Maple, M. Ishikawa, D. G. Hinks, J. D. Jorgensen, G. Saito, and H. Yamochi, Basic similarities among cuprate, bismuthate, organic, chevrel-phase, and heavy-fermion superconductors shown by penetration-depth measurements, *Phys. Rev. Lett.* **68**, 2712 (1992).
- [6] Y. Uemura, Superfluid density of high- T_c cuprate systems: implication on condensation mechanisms, heterogeneity and phase diagram, *Solid State Communications* **126**, 23 (2003), proceedings of the High- T_c Superconductivity Workshop.
- [7] P. W. Anderson, The Resonating Valence Bond State in La_2CuO_4 and Superconductivity, *Science* **235**, 1196 (1987).
- [8] N. Nagaosa and P. A. Lee, Normal-state properties of the uniform resonating-valence-bond state, *Phys. Rev. Lett.* **64**, 2450 (1990).
- [9] P. A. Lee and N. Nagaosa, Gauge theory of the normal state of high- t_c superconductors, *Phys. Rev. B* **46**, 5621 (1992).
- [10] I. Božović, X. He, J. Wu, and A. T. Bollinger, Dependence of the critical temperature in overdoped copper oxides on superfluid density, *Nature* **536**, 309 (2016).
- [11] U. Chatterjee, D. Ai, J. Zhao, S. Rosenkranz, A. Kaminski, H. Raffy, Z. Li, K. Kadowaki, M. Randeria, M. R. Norman, and J. C. Campuzano, Electronic phase diagram of high-temperature copper oxide superconductors, *Proceedings of the National Academy of Sciences* **108**, 9346 (2011).
- [12] K. M. Shen, F. Ronning, D. H. Lu, F. Baumberger, N. J. C. Ingle, W. S. Lee, W. Meevasana, Y. Kohsaka,

- M. Azuma, M. Takano, H. Takagi, and Z.-X. Shen, Nodal quasiparticles and antinodal charge ordering in $\text{Ca}_{2-x}\text{Na}_x\text{CuO}_2\text{Cl}_2$, *Science* **307**, 901 (2005).
- [13] Z.-X. Li, S. A. Kivelson, and D.-H. Lee, Superconductor-to-metal transition in overdoped cuprates, *npj Quantum Materials* **6**, 36 (2021).
- [14] D. Wang, J.-Q. Xu, H.-J. Zhang, and Q.-H. Wang, Anisotropic scattering caused by apical oxygen vacancies in thin films of overdoped high-temperature cuprate superconductors, *Phys. Rev. Lett.* **128**, 137001 (2022).
- [15] N. R. Lee-Hone, J. S. Dodge, and D. M. Broun, Disorder and superfluid density in overdoped cuprate superconductors, *Phys. Rev. B* **96**, 024501 (2017).
- [16] N. R. Lee-Hone, V. Mishra, D. M. Broun, and P. J. Hirschfeld, Optical conductivity of overdoped cuprate superconductors: Application to $\text{La}_{2-x}\text{Sr}_x\text{CuO}_4$, *Phys. Rev. B* **98**, 054506 (2018).
- [17] J. Zaanen, Superconducting electrons go missing, *Nature* **536**, 282 (2016).
- [18] S.-D. Chen, M. Hashimoto, Y. He, D. Song, J.-F. He, Y.-F. Li, S. Ishida, H. Eisaki, J. Zaanen, T. P. Devereaux, D.-H. Lee, D.-H. Lu, and Z.-X. Shen, Unconventional spectral signature of T_c in a pure d-wave superconductor, *Nature* **601**, 562 (2022).
- [19] W. O. Tromp, T. Benschop, J.-F. Ge, I. Battisti, K. M. Bastiaans, D. Chatzopoulos, A. H. M. Vervloet, S. Smit, E. van Heumen, M. S. Golden, Y. Huang, T. Kondo, T. Takeuchi, Y. Yin, J. E. Hoffman, M. A. Sulangi, J. Zaanen, and M. P. Allan, Puddle formation and persistent gaps across the non-mean-field breakdown of superconductivity in overdoped $(\text{Pb,Bi})_2\text{Sr}_2\text{CuO}_{6+\delta}$, *Nature Materials* **22**, 703 (2023).
- [20] S. Pailhès, Y. Sidis, P. Bourges, C. Ulrich, V. Hinkov, L. P. Regnault, A. Ivanov, B. Liang, C. T. Lin, C. Bernhard, and B. Keimer, Two resonant magnetic modes in an overdoped high T_c superconductor, *Phys. Rev. Lett.* **91**, 237002 (2003).
- [21] O. J. Lipscombe, S. M. Hayden, B. Vignolle, D. F. McMorrow, and T. G. Perring, Persistence of high-frequency spin fluctuations in overdoped superconducting $\text{La}_{2-x}\text{Sr}_x\text{CuO}_4$ ($x = 0.22$), *Phys. Rev. Lett.* **99**, 067002 (2007).
- [22] L. Capogna, B. Fauqué, Y. Sidis, C. Ulrich, P. Bourges, S. Pailhès, A. Ivanov, J. L. Tallon, B. Liang, C. T. Lin, A. I. Rykov, and B. Keimer, Odd and even magnetic resonant modes in highly overdoped $\text{Bi}_2\text{Sr}_2\text{CaCu}_2\text{O}_{8+\delta}$, *Phys. Rev. B* **75**, 060502 (2007).
- [23] S. Pailhès, C. Ulrich, B. Fauqué, V. Hinkov, Y. Sidis, A. Ivanov, C. T. Lin, B. Keimer, and P. Bourges, Doping dependence of bilayer resonant spin excitations in $(\text{Y,Ca})\text{Ba}_2\text{Cu}_3\text{O}_{6+x}$, *Phys. Rev. Lett.* **96**, 257001 (2006).
- [24] J. Ayres, M. Berben, M. Čulo, Y.-T. Hsu, E. van Heumen, Y. Huang, J. Zaanen, T. Kondo, T. Takeuchi, J. R. Cooper, C. Putzke, S. Friedemann, A. Carrington, and N. E. Hussey, Incoherent transport across the strange-metal regime of overdoped cuprates, *Nature* **595**, 661 (2021).
- [25] Z.-Y. Weng, Superconducting ground state of a doped mott insulator, *New Journal of Physics* **13**, 103039 (2011).
- [26] Y. Ma, P. Ye, and Z.-Y. Weng, Low-temperature pseudogap phenomenon: precursor of high- T_c superconductivity, *New J. Phys.* **16**, 083039 (2014).
- [27] J. W. Mei and Z. Y. Weng, Spin-roton excitations in the cuprate superconductors, *Physical Review B* **81**, 014507 (2010).
- [28] D. N. Sheng, Y. C. Chen, and Z. Y. Weng, Phase String Effect in a Doped Antiferromagnet, *Phys. Rev. Lett.* **77**, 5102 (1996).
- [29] Z. Y. Weng, D. N. Sheng, Y.-C. Chen, and C. S. Ting, Phase string effect in the t - j model: General theory, *Phys. Rev. B* **55**, 3894 (1997).
- [30] K. Wu, Z. Y. Weng, and J. Zaanen, Sign structure of the t - J model, *Phys. Rev. B* **77**, 155102 (2008).
- [31] S.-P. Kou and Z.-Y. Weng, Topological gauge structure and phase diagram for weakly doped antiferromagnets, *Phys. Rev. Lett.* **90**, 157003 (2003).
- [32] S.-P. Kou, X.-L. Qi, and Z.-Y. Weng, Mutual Chern-Simons effective theory of doped antiferromagnets, *Phys. Rev. B* **71**, 235102 (2005).
- [33] P. Ye, C.-S. Tian, X.-L. Qi, and Z.-Y. Weng, Confinement-Deconfinement Interplay in Quantum Phases of Doped Mott Insulators, *Phys. Rev. Lett.* **106**, 147002 (2011), 1007.2507.
- [34] Z.-J. Song, J.-X. Zhang, and Z.-Y. Weng, Thermal Hall effect and neutral spinons in a doped Mott insulator, *Physical Review Research* **6**, 023328 (2024).
- [35] C. Chen, J.-X. Zhang, Z.-J. Song, and Z.-Y. Weng, Non-ijoffe-larkin composition rule and spinon-dictated electric transport in doped mott insulators, arXiv preprint arXiv:2406.15553 (2024).
- [36] J.-X. Zhang, C. Chen, J.-H. Zhang, and Z.-Y. Weng, Hourglasslike spin excitation in a doped mott insulator, *Phys. Rev. Res.* **6**, 013109 (2024).
- [37] S. Pailhès, Y. Sidis, P. Bourges, V. Hinkov, A. Ivanov, C. Ulrich, L. P. Regnault, and B. Keimer, Resonant Magnetic Excitations at High Energy in Superconducting $\text{YBa}_2\text{Cu}_3\text{O}_{6.85}$, *Phys. Rev. Lett.* **93**, 167001 (2004).
- [38] S. M. Hayden, H. A. Mook, P. Dai, T. G. Perring, and F. Dogan, The structure of the high-energy spin excitations in a high-transition-temperature superconductor, *Nature* **429**, 531 (2004).
- [39] W. Q. Chen and Z. Y. Weng, Spin dynamics in a doped-mott-insulator superconductor, *Phys. Rev. B* **71**, 134516 (2005).
- [40] Z. Y. Weng, D. N. Sheng, and C. S. Ting, Mean-field description of the phase string effect in the $t - j$ model, *Phys. Rev. B* **59**, 8943 (1999).
- [41] J. B. Kogut, An introduction to lattice gauge theory and spin systems, *Rev. Mod. Phys.* **51**, 659 (1979).

Supplementary Materials for: “Intrinsic phase fluctuation and superfluid density in doped Mott insulators”

CONTENTS

Acknowledgments	5
References	5
A. Derivation of the effective Lagrangian	7
1. Effective Model for Dynamics of A^s	7
2. Effective Model for External Response: From Eq. (10) to Eq. (11)	9
B. Mean-field theory of b -spinon	9
C. Renormalization group analysis of the superconducting transition	11

Appendix A: Derivation of the effective Lagrangian

1. Effective Model for Dynamics of A^s

The Lagrangian of the mutual Chern-Simons gauge theory reads $L = L_s + L_h + L_{\text{MCS}}$, where

$$\begin{aligned}
L_h &= \sum_i h_i^\dagger [\partial_0 - iA_0^s(i) - iA_0^e(i) + \mu_h] h_i - t_h \sum_{i,\alpha} \left[h_i^\dagger h_{i+\alpha} e^{i\mathbf{A}_\alpha^s(i) + i\mathbf{A}_\alpha^e(i)} + \text{H.c.} \right], \\
L_s &= \sum_{i,\sigma} b_{i,\sigma}^\dagger [\partial_0 - i\sigma A_0^h(i) + \lambda_b] b_{i,\sigma} - \frac{J_s}{2} \sum_{i,\alpha,\sigma} \left[b_{i,\sigma}^\dagger b_{i+\alpha,-\sigma}^\dagger e^{i\sigma \mathbf{A}_\alpha^h(i)} + \text{H.c.} \right], \\
L_{\text{MCS}} &= \frac{i}{\pi} \sum_i \epsilon^{\mu\nu\lambda} A_\mu^s(i) \partial_\nu A_\lambda^h(i) = \frac{i}{\pi} \sum_i A_0^s(i) \mathbf{B}^h(i) - \sum_i \frac{i}{\pi} \mathbf{A}^s(i) \cdot (\mathbf{E}^h(i) \times \hat{z})
\end{aligned}$$

represent the holon action, spinon action and the mutual Chern-Simons term respectively. Integrating out spinon matter field b and b^\dagger , leads to an effective action S_{eff}

$$Z = \int D[h^\dagger, h] D[b^\dagger, b] D\mathbf{A}^s D\mathbf{A}^h \exp \left[- \int_0^\beta d\tau (L_h + L_s + L_{\text{MCS}}) \right] = \int D[h^\dagger, h] D\mathbf{A}^s D\mathbf{A}^h \exp(-S_{\text{eff}}) \quad (\text{AS1})$$

where

$$S_{\text{eff}} = \frac{1}{2} \sum_{i\omega_n} \int d^2\mathbf{q} A_\mu^h(\mathbf{q}, i\omega_n) \Pi_{\mu\nu}^s(\mathbf{q}, i\omega_n) A_\nu^h(-\mathbf{q}, -i\omega_n) + \int_0^\beta d\tau L_h + \int_0^\beta d\tau L_{\text{MCS}} \quad (\text{AS2})$$

and the information of the b -spinon matter field is encoded in the polarization tensors defined as:

$$\begin{aligned}
\Pi_{00}^s(\mathbf{q}, i\omega_n) &= \sum_{\sigma\sigma'} \sigma\sigma' \langle n_\sigma^b(\mathbf{q}, i\omega_n) n_{\sigma'}^b(-\mathbf{q}, -i\omega_n) \rangle = 4 \langle S^z(\mathbf{q}, i\omega_n) S^z(-\mathbf{q}, -i\omega_n) \rangle = 4\chi^{zz}(\mathbf{q}, i\omega_n) \\
\Pi_{0\alpha}^s(\mathbf{q}, i\omega_n) &= \sum_\sigma 2\sigma \langle n_\sigma^b(\mathbf{q}, i\omega_n) j_\alpha^{s,(P)}(-\mathbf{q}, -i\omega_n) \rangle \\
\Pi_{\alpha\beta}^s(\mathbf{q}, i\omega_n) &= \Pi_{\alpha\beta}^{s,(P)}(\mathbf{q}, i\omega_n) + \Pi_{\alpha\beta}^{s,(D)}(\mathbf{q}, i\omega_n) = 4 \langle j_\alpha^{s,(P)}(\mathbf{q}, i\omega_n) j_\beta^{s,(P)}(-\mathbf{q}, -i\omega_n) \rangle + 2 \left\langle \frac{\partial j_\alpha^{s,(D)}(\mathbf{q}, i\omega_n)}{\partial \delta A_\alpha^h} \right\rangle \delta_{\alpha\beta}.
\end{aligned} \quad (\text{AS3})$$

In the above derivation, $S^z(\mathbf{q}, i\omega)$ is the Fourier transformation of the spinon spin operator $S_i^z = \frac{1}{2}(b_{i,\uparrow}^\dagger b_{i,\uparrow} - b_{i,\downarrow}^\dagger b_{i,\downarrow})$, $j_\alpha^{s,(P)}(\mathbf{q}, i\omega)$ and $j_\alpha^{s,(D)}(\mathbf{q}, i\omega)$ are the Fourier transformation of the paramagnetic and diamagnetic components of the total spinon current $j_{i\alpha}^s$, defined as:

$$\begin{aligned} j_{i\alpha}^{s,(P)} &= \frac{\partial L_s[\bar{\mathbf{A}}^h + \delta \mathbf{A}^h]}{\partial \delta A_{i\alpha}^h} = i \frac{J_s}{2} \sum_{\sigma} \left(\sigma b_{i+\alpha,\sigma}^\dagger b_{i,\sigma}^\dagger e^{i\sigma \bar{A}_{i\alpha}^h} - \text{H.c.} \right), \\ j_{i\alpha}^{s,(D)} &= \frac{\partial^2 L_s}{\partial A_{i\alpha}^h \partial A_{i\beta}^h} \delta A_{i\alpha}^h = -\frac{J_s}{2} \sum_{\sigma} \left(b_{i+\alpha,\sigma}^\dagger b_{i,\sigma}^\dagger e^{i\sigma \bar{A}_{i\alpha}^h} + \text{H.c.} \right), \\ j_{i\alpha}^s &= j_{i\alpha}^{s,(P)} + j_{i\alpha}^{s,(D)}. \end{aligned} \quad (\text{AS4})$$

When spinons are in the normal state (no spinon condensate, no antiferromagnetic long-range order), spinon current conserves due to the $U(1)$ gauge symmetry of \mathbf{A}^h . We expect a Maxwell term of \mathbf{E}^h and \mathbf{B}^h in the effective gauge theory. Conservation of spinon current $\partial_\mu j_\mu^s = 0$ gives constraints on polarization tensors $\partial_\mu \Pi_{\mu\nu}^s = 0$, which is detailed in the momentum space at long wavelength limit in the following,

$$\Pi_{00}^s = q^2 \Pi_0^s, \quad (\text{AS5})$$

$$\Pi_{0\alpha}^s = (i\omega_n) q_\alpha \Pi_0^s + i\epsilon^{\alpha\beta} q_\beta \Pi_1^s, \quad (\text{AS6})$$

$$\Pi_{\alpha 0}^s = (i\omega_n) q_\alpha \Pi_0^s - i\epsilon^{\alpha\beta} q_\beta \Pi_1^s, \quad (\text{AS7})$$

$$\Pi_{\alpha\beta}^s = \delta_{\alpha\beta} (i\omega_n)^2 \Pi_0^s - i\epsilon^{\alpha\beta} \omega_n \Pi_1^s + (\delta_{\alpha\beta} q^2 - q_\alpha q_\beta) \Pi_2^s. \quad (\text{AS8})$$

Without polarization due to external magnetic field, time reversal symmetry remains intact, then $\Pi_1^s = 0$. S_{eff} now contains only a Maxwell term,

$$S_{\text{eff}} = \int_0^\beta d\tau \int d\mathbf{r} \left(\frac{1}{2} \Pi_0^s \mathbf{E}^h \cdot \mathbf{E}^h + \frac{1}{2} \Pi_2^s \mathbf{B}^h \cdot \mathbf{B}^h \right) + \int_0^\beta d\tau (L_h + L_{MCS}) \quad (\text{AS9})$$

One step further, integrating out internal fields \mathbf{E}^h and \mathbf{B}^h , we have

$$\int D\mathbf{E}^h D\mathbf{B}^h \exp(-S_{\text{eff}}) = \exp \left[- \int_0^\beta d\tau \int d\mathbf{r} \left[\frac{1}{2\pi^2} \frac{1}{\Pi_0^s} (A_\alpha^s)^2 + \frac{1}{2\pi^2} \frac{1}{\Pi_2^s} (A_0^s)^2 \right] + \int_0^\beta d\tau L_h \right]. \quad (\text{AS10})$$

We are not going to consider the compressibility or response to chemical potential here, thus we take the gapped $A_0^s = 0$ fixed at saddle point. Recall that $\Pi_0^s = \frac{\Pi_{00}^s}{q^2}$, integrating over A^h and b -spinon leads to an additional term of A^s in the action, which reads

$$\begin{aligned} \int_0^\beta d\tau \int d\mathbf{r} \frac{1}{2\pi^2} \frac{1}{\Pi_0^s} (A_\alpha^s)^2 &= \int_0^\beta d\tau \int d\mathbf{r} \frac{1}{2} \frac{1}{\pi^2} \left(\frac{\Pi_{00}^s}{q^2} \right)^{-1} (A_\alpha^s)^2 = \int_0^\beta d\tau \int d\mathbf{r} \frac{1}{2} \left(\frac{4\pi^2 \langle S^z S^z \rangle}{q^2} \right)^{-1} (A_\alpha^s)^2 \\ &= \int_0^\beta d\tau \int d\mathbf{r} \frac{1}{2} \left(\frac{4\pi^2 \chi^{zz}(q)}{q^2} \right)^{-1} (A_\alpha^s)^2 = \int_0^\beta d\tau \int d\mathbf{r} \frac{1}{2} (D_{\alpha\alpha}^{A_s})^{-1} (A_\alpha^s)^2. \end{aligned} \quad (\text{AS11})$$

This can be understood as the equivalence between single spin excitation and the related flux $\mathbf{B}^s = \pi \sum_\sigma \sigma n_\sigma^b = 2\pi S^z$:

$$\begin{aligned} \chi^{zz}(\mathbf{q}, i\omega_n) &\equiv \langle S^z(\mathbf{q}, i\omega_n) S^z(-\mathbf{q}, -i\omega_n) \rangle = \frac{1}{4\pi^2} \langle \mathbf{B}^s(\mathbf{q}, i\omega_n) \mathbf{B}^s(-\mathbf{q}, -i\omega_n) \rangle \\ &= \frac{1}{4\pi^2} \left(q_x^2 \langle A_y^s(\mathbf{q}, i\omega_n) A_y^s(-\mathbf{q}, -i\omega_n) \rangle + q_y^2 \langle A_x^s(\mathbf{q}, i\omega_n) A_x^s(-\mathbf{q}, -i\omega_n) \rangle - 2q_x q_y \langle A_x^s(\mathbf{q}, i\omega_n) A_y^s(-\mathbf{q}, -i\omega_n) \rangle \right) \\ &= \frac{1}{4\pi^2} q^2 D_{\alpha\alpha}^{A_s}, \end{aligned} \quad (\text{AS12})$$

where $D_{\alpha\beta}^{A_s} \equiv \langle A_\alpha^s A_\beta^s \rangle$ denotes the propagator of gauge field \mathbf{A}^s , and isotropy provides that $D_{\alpha\beta}^{A_s} = \delta_{\alpha\beta} D_{\alpha\alpha}^{A_s}$. We see this relation exactly maps to the effective Lagrangian derived by field integration of spinon Eq. (AS11).

2. Effective Model for External Response: From Eq. (10) to Eq. (11)

In the long wavelength limit, the effective action of holon and \mathbf{A}^s reads,

$$\begin{aligned} S &= \frac{1}{2} \int_0^\beta d\tau \int d\mathbf{r} \rho_s^0 (\partial_\alpha \theta^h - A_\alpha^s - A_\alpha^{\text{ext}})^2 + \int_0^\beta d\tau \int d\mathbf{r} \frac{1}{2} (D_{\alpha\alpha}^{A_s})^{-1} (A_\alpha^s)^2 \\ &= \frac{1}{2} \int_0^\beta d\tau \int d\mathbf{r} [\rho_s^0 (\partial_\alpha \theta^h - A_\alpha^s - A_\alpha^{\text{ext}})^2 + \lambda E_g A_\alpha^s{}^2], \end{aligned} \quad (\text{AS13})$$

where $\rho_0^s = 2t_h n^h = 2t_h \delta$, the equilibrium is given by the saddle point equation of internal gauge field A^s after fixing the gauge to eliminate the matter field,

$$\frac{\delta S}{\delta A_\alpha^s} = 0 \quad \Rightarrow \quad A_\alpha^s = -\frac{\rho_0^s}{\rho_0^s + \lambda E_g} A_\alpha^{\text{ext}}. \quad (\text{AS14})$$

Physically, the minus sign implies that the external field A^{ext} is screened by the internal gauge field A^s . Put this saddle point back to Eq. (10), we arrive at the effective action for external field:

$$S_{\text{ext}}[A_\alpha^{\text{ext}}] = \frac{1}{2} \int_0^\beta d\tau \int d\mathbf{r} \rho_0^s \frac{\lambda E_g}{\rho_0^s + \lambda E_g} (A_\alpha^{\text{ext}})^2. \quad (\text{AS15})$$

Besides using the saddle point method, similar result can also be obtained by integrating over \mathbf{A}^s .

Appendix B: Mean-field theory of b -spinon

The b -spinon ground state and excitations are described by the following Hamiltonian,

$$H_s = -J_s \sum_{i,\alpha,\sigma} \left(b_{i+\alpha,\sigma}^\dagger b_{i,-\sigma}^\dagger e^{i\sigma A_{i\alpha}^h} + h.c. \right) + \lambda_b \sum_\sigma b_{i,\sigma}^\dagger b_{i,\sigma} + \text{const.}, \quad (\text{BS1})$$

where $\alpha = \hat{x}, \hat{y}$, $J_s = J_{\text{eff}} \Delta^s / 2$ and J_{eff} is the effective super-exchange in [26]. We take the convention of the Fourier transform as

$$b_{i,\sigma} = \frac{1}{\sqrt{N}} \sum_{\mathbf{k}} e^{-i\mathbf{k}\cdot\mathbf{r}_i} b_{\mathbf{k},\sigma}, \quad \mathbf{k} \in \text{BZ}. \quad (\text{BS2})$$

The Hamiltonian can be diagonalized, with the notification that each plaquette is attached with $\delta\pi$ flux through the gauge field $A_{i\alpha}^h = A_{i+\alpha,i}^h$ generated by the uniformly condensed holons ($\delta = 2p/q$, p and q are coprime integers). By choosing the gauge field on each bond as $(A_{ix}^h, A_{iy}^h) = (0, Q i_x)$, where $Q = \delta\pi$ and i_x labels the horizontal position of site i , the Hamiltonian can be written in momentum space as

$$H_s = \sum_{\mathbf{k} \in \text{MBZ}} \begin{pmatrix} \phi_{\mathbf{k},\uparrow}^\dagger & \phi_{-\mathbf{k},\downarrow} \end{pmatrix} \begin{pmatrix} \lambda_b I & K \\ K & \lambda_b I \end{pmatrix} \begin{pmatrix} \phi_{\mathbf{k},\uparrow} \\ \phi_{-\mathbf{k},\downarrow}^\dagger \end{pmatrix} \quad (\text{BS3})$$

where

$$\begin{aligned} \phi_{\mathbf{k},\uparrow} &= (b_{\mathbf{k}-Q\hat{x},\uparrow}, \dots, b_{\mathbf{k}-(q-1)Q\hat{x},\uparrow}, b_{\mathbf{k}-qQ\hat{x},\uparrow})^T, \\ \phi_{-\mathbf{k},\downarrow} &= (b_{-\mathbf{k}+Q\hat{x},\downarrow}, \dots, b_{-\mathbf{k}+(q-1)Q\hat{x},\downarrow}, b_{-\mathbf{k}+qQ\hat{x},\downarrow}), \end{aligned} \quad (\text{BS4})$$

I is the identity matrix and

$$K = -\frac{J_{\text{eff}} \Delta^s}{2} \begin{pmatrix} 2 \cos(k_x - Q) & e^{-iky} & 0 & e^{iky} \\ e^{iky} & 2 \cos(k_x - 2Q) & e^{-iky} & 0 \\ 0 & e^{iky} & \dots & e^{-iky} \\ e^{-iky} & 0 & e^{iky} & 2 \cos(k_x - qQ) \end{pmatrix}. \quad (\text{BS5})$$

$\sum_{\mathbf{k} \in \text{MBZ}}$ denotes a summation over the magnetic Brillouin zone (MBZ), which arises due to the reduced translational symmetry imposed by the flux.

The b -spinon can be transformed first using

$$\begin{aligned}\phi_{\mathbf{k},\uparrow} &= \sum_r \omega_r(\mathbf{k}) \beta_{r,\mathbf{k},\uparrow}, \\ \phi_{-\mathbf{k},\downarrow}^\dagger &= \sum_r \omega_r(\mathbf{k}) \beta_{r,-\mathbf{k},\downarrow}^\dagger.\end{aligned}\tag{BS6}$$

where, $\omega_r(\mathbf{k})$ is the r -th eigenvector of K matrix, satisfying the eigen-equation

$$K\omega_r(\mathbf{k}) = \omega_r(\mathbf{k})\xi_{r,\mathbf{k}}.\tag{BS7}$$

Then the Hamiltonian reads

$$H_s = \sum_r \sum_{\mathbf{k} \in \text{MBZ}} \begin{pmatrix} \beta_{r,\mathbf{k},\uparrow}^\dagger & \beta_{r,-\mathbf{k},\downarrow} \end{pmatrix} \begin{pmatrix} \lambda_b & \xi_{r,\mathbf{k}} \\ \xi_{r,\mathbf{k}} & \lambda_b \end{pmatrix} \begin{pmatrix} \beta_{r,\mathbf{k},\uparrow} \\ \beta_{r,-\mathbf{k},\downarrow}^\dagger \end{pmatrix}.\tag{BS8}$$

The fully diagonalized Hamiltonian reads

$$H_s = \sum_{r,\mathbf{k},\sigma} E_{r,\mathbf{k}} \gamma_{r,\mathbf{k},\sigma}^\dagger \gamma_{r,\mathbf{k},\sigma} + \text{const.}\tag{BS9}$$

with

$$\begin{aligned}E_{r,\mathbf{k}} &= \sqrt{\lambda_b^2 - \xi_{r,\mathbf{k}}^2} \\ \begin{pmatrix} \gamma_{r,\mathbf{k},\uparrow} \\ \gamma_{r,-\mathbf{k},\downarrow}^\dagger \end{pmatrix} &= \begin{pmatrix} u_{r,\mathbf{k}} & v_{r,\mathbf{k}} \\ v_{r,\mathbf{k}} & u_{r,\mathbf{k}} \end{pmatrix} \begin{pmatrix} \beta_{r,\mathbf{k},\uparrow} \\ \beta_{r,-\mathbf{k},\downarrow}^\dagger \end{pmatrix}\end{aligned}\tag{BS10}$$

where, the coherent factors $u_{r,\mathbf{k}}$ and $v_{r,\mathbf{k}}$ read

$$\begin{aligned}u_{r,\mathbf{k}} &= \frac{1}{\sqrt{2}} \sqrt{1 + \frac{\lambda_b}{E_{r,\mathbf{k}}}} \\ v_{r,\mathbf{k}} &= \frac{1}{\sqrt{2}} \text{sgn}(\xi_{r,\mathbf{k}}) \sqrt{-1 + \frac{\lambda_b}{E_{r,\mathbf{k}}}}.\end{aligned}\tag{BS11}$$

The mean-field self-consistent equations are derived by finding the saddle point of the free energy,

$$F(\lambda_b, \Delta^s) = \sum_{r,\mathbf{k}} \left[E_{r,\mathbf{k}} + \frac{2}{\beta} \ln(1 - e^{-\beta E_{r,\mathbf{k}}}) \right] - 2\lambda_b N + J_{\text{eff}} (\Delta^s)^2 N,\tag{BS12}$$

whose saddle point equations read

$$\begin{aligned}\sum_{r,\mathbf{k}} \frac{\lambda_b}{E_{r,\mathbf{k}}} \coth\left(\frac{\beta E_{r,\mathbf{k}}}{2}\right) &= 2N, \\ \sum_{r,\mathbf{k}} \frac{J_{\text{eff}} \xi_{r,\mathbf{k}}^2}{4E_{r,\mathbf{k}}} \coth\left(\frac{\beta E_{r,\mathbf{k}}}{2}\right) &= 2N.\end{aligned}\tag{BS13}$$

Following the above derivation, the Fourier transformation of S_i reads

$$\begin{aligned}S(\mathbf{q}) &= \frac{1}{2} \sum_{\mathbf{k}} (b_{\mathbf{k},\uparrow}^\dagger b_{\mathbf{k}+\mathbf{q},\uparrow} - b_{\mathbf{k},\downarrow}^\dagger b_{\mathbf{k}+\mathbf{q},\downarrow}) \\ &= \frac{1}{2} \sum_{\mathbf{k} \in \text{MBZ}} \sum_{m,n} \omega_m^\dagger(\mathbf{k}) \omega_n(\mathbf{k} + \mathbf{q}) \begin{pmatrix} \beta_{m,\mathbf{k},\uparrow}^\dagger & \beta_{m,-\mathbf{k},\downarrow} \end{pmatrix} \begin{pmatrix} 1 & 0 \\ 0 & -1 \end{pmatrix} \begin{pmatrix} \beta_{n,\mathbf{k}+\mathbf{q},\uparrow} \\ \beta_{n,-\mathbf{k}-\mathbf{q},\downarrow}^\dagger \end{pmatrix}.\end{aligned}\tag{BS14}$$

The spin susceptibility is defined in [39, 40], which reads

$$\chi^{zz}(\mathbf{q}, \tau) = \frac{1}{N\beta} \langle \hat{T} S(\mathbf{q}, \tau)^z S(-\mathbf{q}, 0) \rangle_0^c\tag{BS15}$$

where $\langle \hat{O} \rangle_0$ denotes the expectation value of \hat{O} under the mean-field quadratic Hamiltonian, superscript c denotes the connected contraction. The Green function of Bogoliubov quasi-particle follows directly from Eq.(BS9)

$$\begin{aligned} \chi^{zz}(\mathbf{q}, \tau) &= \frac{1}{4N} \sum_{\mathbf{k}, m, n} |\omega_m^\dagger(\mathbf{k}) w_n(\mathbf{k} + \mathbf{q})|^2 \cdot \\ &[(u_{m, \mathbf{k}} v_{n, \mathbf{k} + \mathbf{q}} - v_{m, \mathbf{k}} u_{n, \mathbf{k} + \mathbf{q}})^2 (e^{-\tau(E_{m, \mathbf{k}} + E_{n, \mathbf{k} + \mathbf{q}})} (1 + n_{n, \mathbf{k}})(1 + n_{n, \mathbf{k} + \mathbf{q}}) + e^{\tau(E_{m, \mathbf{k}} + E_{n, \mathbf{k} + \mathbf{q}})} n_{m, \mathbf{k}} n_{n, \mathbf{k} + \mathbf{q}}) \\ &+ (u_{m, \mathbf{k}} u_{n, \mathbf{k} + \mathbf{q}} - v_{m, \mathbf{k}} v_{n, \mathbf{k} + \mathbf{q}})^2 (e^{\tau(E_{m, \mathbf{k}} - E_{n, \mathbf{k} + \mathbf{q}})} n_{m, \mathbf{k}} (1 + n_{n, \mathbf{k} + \mathbf{q}}) + e^{\tau(-E_{m, \mathbf{k}} + E_{n, \mathbf{k} + \mathbf{q}})} (1 + n_{m, \mathbf{k} + \mathbf{q}}) n_{n, \mathbf{k} + \mathbf{q}})], \end{aligned} \quad (\text{BS16})$$

The spin susceptibility in the frequency domain can be obtained,

$$\begin{aligned} \chi^{zz}(\mathbf{q}, i\omega_n) &= \frac{1}{4N} \sum_{\mathbf{k}, m, n} |\omega_m^\dagger(\mathbf{k}) w_n(\mathbf{k} + \mathbf{q})|^2 [(1 - \frac{\lambda^2 - \xi_{m, \mathbf{k}} \xi_{n, \mathbf{k} + \mathbf{q}}}{E_{m, \mathbf{k}} E_{n, \mathbf{k} + \mathbf{q}}}) \frac{E_{m, \mathbf{k}} + E_{n, \mathbf{k} + \mathbf{q}}}{(i\omega_n)^2 - (E_{m, \mathbf{k}} + E_{n, \mathbf{k} + \mathbf{q}})^2} (1 + n_{m, \mathbf{k}} + n_{n, \mathbf{k} + \mathbf{q}}) \\ &+ (1 + \frac{\lambda^2 - \xi_{m, \mathbf{k}} \xi_{n, \mathbf{k} + \mathbf{q}}}{E_{m, \mathbf{k}} E_{n, \mathbf{k} + \mathbf{q}}}) \frac{-E_{m, \mathbf{k}} + E_{n, \mathbf{k} + \mathbf{q}}}{(i\omega_n)^2 - (E_{m, \mathbf{k}} + E_{n, \mathbf{k} + \mathbf{q}})^2} (-n_{m, \mathbf{k}} + n_{n, \mathbf{k} + \mathbf{q}})]. \end{aligned} \quad (\text{BS17})$$

At zero temperature,

$$\begin{aligned} \chi^{zz}(\mathbf{q}, i\omega_n) &= \frac{1}{4N} \sum_{\mathbf{k}, m, n} |\omega_m^\dagger(\mathbf{k}) w_n(\mathbf{k} + \mathbf{q})|^2 [(1 - \frac{\lambda^2 - \xi_{m, \mathbf{k}} \xi_{n, \mathbf{k} + \mathbf{q}}}{E_{m, \mathbf{k}} E_{n, \mathbf{k} + \mathbf{q}}}) \frac{E_{m, \mathbf{k}} + E_{n, \mathbf{k} + \mathbf{q}}}{(i\omega_n)^2 - (E_{m, \mathbf{k}} + E_{n, \mathbf{k} + \mathbf{q}})^2} \\ &= \frac{1}{8N} \sum_{\mathbf{k}, m, n} |\omega_m^\dagger(\mathbf{k}) w_n(\mathbf{k} + \mathbf{q})|^2 [(1 - \frac{\lambda^2 - \xi_{m, \mathbf{k}} \xi_{n, \mathbf{k} + \mathbf{q}}}{E_{m, \mathbf{k}} E_{n, \mathbf{k} + \mathbf{q}}}) (\frac{1}{i\omega_n - E_{m, \mathbf{k}} - E_{n, \mathbf{k} + \mathbf{q}}} - \frac{1}{i\omega_n + E_{m, \mathbf{k}} + E_{n, \mathbf{k} + \mathbf{q}}})]. \end{aligned} \quad (\text{BS18})$$

In the main text, we utilize the low-energy, low-frequency scaling of $\text{Re} \chi^{zz}(q, \omega)$ as q^2/E_g . This understanding is straightforward. The b -spinons form a nearly dispersionless, Landau-level-like spectrum in momentum space, where the low-energy fluctuations are primarily governed by the lowest energy level E_g . In other words, E_g is the only relevant energy scale in this regime. We can also verify this numerically as shown in Fig. BS1. The mean-field result is carried out for $t = 2J$.

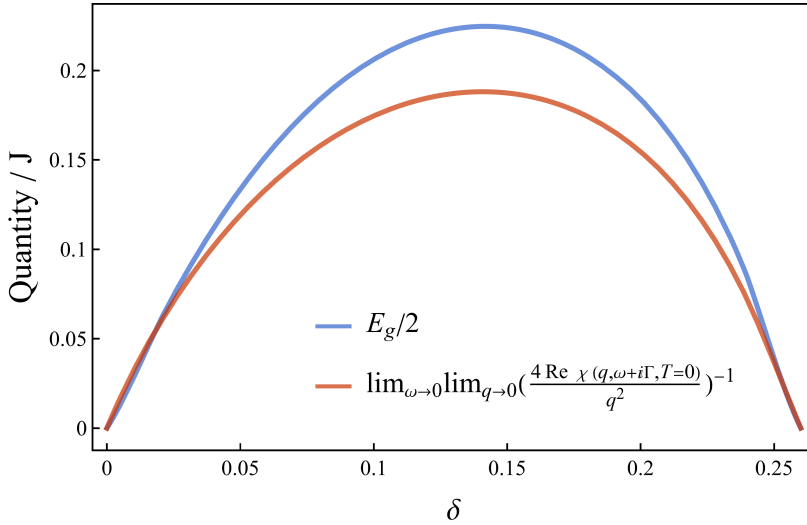


FIG. BS1. The low momentum, low frequency scaling of $\text{Re} \chi^{zz}$. Numerically, we show that the scaling behavior is q^2 , with a proportionality constant.

Appendix C: Renormalization group analysis of the superconducting transition

The Lagrangian of holons is written below,

$$L_h = \sum_i h_i^\dagger [\partial_\tau - iA_0^s(i) - iA_0^e(i)] h_i - t_h \sum_{\langle ij \rangle} (h_i^\dagger h_j e^{iA_{ij}^s} + \text{h.c.}) + \mu (\sum_i h_i^\dagger h_i - N\delta) + \frac{u}{2} \sum_i n_i^2, \quad (\text{CS1})$$

where the onsite repulsion term $\frac{u}{2} \sum_i n_i^2$ is introduced in order to properly describe the hard-core nature of the holons. In the superconducting phase, holons condense uniformly, allowing us to express h_i as $\sqrt{n_i} e^{i\theta_i}$, where $\sqrt{n_i}$ and θ_i represent the amplitude and phase respectively. In the long-wavelength limit, we have

$$L_h = \sum_i n_i^h [\partial_\tau \theta(i) - iA_0^s(i) - iA_0^e(i)] - 2t_h n_i^h \cos(\partial_\alpha \theta(i) - A_\alpha^s(i) - A_\alpha^e(i)) + \mu (\sum_i h_i^\dagger h_i - N\delta) + \frac{u}{2} \sum_i n_i^2. \quad (\text{CS2})$$

Using the Villian expansion,

$$e^{\beta \cos x} = \text{const.} \sum_{N_\alpha \in \mathbf{Z}} \exp \left[-\frac{\beta}{2} (x - 2\pi N_\alpha)^2 \right], \quad (\text{CS3})$$

and expanding the holon density around its saddle point, $n_i^h = \bar{n}^h + \delta n_i^h$, the action can be expanded up to order $O(\delta n^2, \delta \theta^2)$. After integrating out the holon density fluctuation, we have

$$L_h + L_{\text{MCS}} = \sum_i \left\{ \frac{1}{2u} [\partial_\tau \theta(i) - iA_0^s(i) - iA_0^e(i)]^2 + \bar{n}_i^h (\partial_\tau \theta(i) - iA_0^s(i) - iA_0^e(i)) \right. \\ \left. + t_h \bar{n}_i^h (\partial_\alpha \theta(i) - A_\alpha^s(i) - eA_\alpha^s(i) + 2\pi N_\alpha) + \frac{i}{\pi} A_0^s(i) \mathbf{B}^h(i) - \frac{i}{\pi} \mathbf{A}^s(i) \cdot (\mathbf{E}^h(i) \times \hat{z}) \right\}. \quad (\text{CS4})$$

Performing a gauge transformation to eliminate the holon phase field, $A_\alpha^s \rightarrow A_\alpha^s - \partial_\alpha \theta$, $iA_0^s \rightarrow iA_0^s - \partial_\tau \theta$, and integrating out \mathbf{A}^s , we have arrived at the effective Lagrangian describing the physics of the holon vortex coupled to the holon gauge field,

$$L_{\text{eff}} = \frac{u}{2\pi^2} \sum_i (B^h - \pi \bar{n}_i^h)^2 + \sum_i \frac{1}{4\pi^2 t_h \bar{n}_h} (E_\alpha^h)^2 - \frac{i}{\pi} \sum_i \epsilon^{\mu\nu\lambda} A_\mu^e \partial_\nu A_\lambda^h - 2i \sum_i A_\mu^h J_\mu^{\text{vor}}, \quad (\text{CS5})$$

where J_μ^{vor} captures the singular part of the phase θ , $J_0^{\text{vor}} = \epsilon^{\alpha\beta} \partial_\alpha N_\beta$, $J_\alpha^{\text{vor}} = -\epsilon^{\alpha\beta} \partial_0 N_\beta$. The above derivation closely follows the standard particle-vortex duality transformation [41]. To figure out the interaction among the vortices. We start by integrating out A_0^h which couples to the vortex density directly. Recall that A_0^h couples to b -spinon spins as well, we need to combine L_{eff} and L_s . The integration leads to

$$L_{\text{vor}} = -\frac{t_h \bar{n}^h \pi}{2} \sum_{i,j} Q_i \frac{\ln(r_i - r_j)}{a} Q_j, \quad (\text{CS6})$$

where $Q_i = 2J_0^{\text{vor}}(i) + \sum_\sigma \sigma b_{i\sigma}^\dagger b_{i\sigma}$ is the effective vorticity, combining the $\pm\pi$ flux spinon and the $\mp 2\pi$ flux holon vortex. Since the vortex carries a singular self-energy, we restrict ourselves to consider the system with zero total vorticity. The now composite objects called spinon-vortices interact with each other through a logarithmic interaction similar to the 2-dimensional electron gas.

Since each spin-vortex contains a spinon excitation inside the core, we need to consider the excitation energy of the spinon $E_g/2$ as the self energy of the spinon-vortex, and only consider the vorticity $Q_i = \pm 1$. The effective action of the system now reads

$$S_{\text{eff}} = \frac{E_g}{2k_B T} \sum_i |Q_i| - \pi \frac{K}{4} \sum_{i,j} Q_i \frac{\ln(r_i - r_j)}{a} Q_j \quad (\text{CS7})$$

where $K = \frac{2t_h \bar{n}^h}{k_B T}$ is the reduced stiffness and the fugacity is $y = e^{-E_g/2k_B T}$.

Following the textbook level derivation of the Kosterlitz-Thouless transition, we can derive the corresponding RG equations of stiffness and fugacity,

$$\frac{dK^{-1}}{dl} = g^2 \pi^3 y^2 + O(y^4), \\ \frac{dy}{dl} = (2 - \pi \frac{K}{4}) y + O(y^3). \quad (\text{CS8})$$

Here, y is replaced by gy . $g = 4$ represents the 4-fold degeneracy of each site on the von Neumann lattice, arising from time reversal and bipartite lattice symmetries [26]. The replacement of K by $K/4$ contrary to the standard KT analysis reflects the π vorticity of each spinon vortex instead of 2π . The transition occurs at $(K^*, y^*) = (8/\pi, 0)$. Correspondingly, the transition temperature T_c satisfies

$$\frac{E_g}{k_B T_c} = 2 \ln(8\pi) \approx 6.44. \quad (\text{CS9})$$